The Pharmaceutical and Chemical Journal, 2023, 10(6):25-36

Available online www.tpcj.org

Research Article

ISSN: 2349-7092
CODEN(USA): PCJHBA

Purine analogs Synthesis, Molecular Docking Studies and ADME Properties of Some New Pyrazolo[1,5-a]pyrimidines and Evaluation of their Antimicrobial and Anticancer Activities as CDK inhibitors

Haytham E. Dweedar[1], Hoda Mahrous[1], Noha Sorour[1], Omar A. Ahmed-Farid[2]

[1]Industrial Biotechnology Department, Genetic Engineering and Biotechnology Research Institute (GEBRI), Sadat City University, Egypt
[2]Physiology Department, National Organization for Drug Control and Research (NODCAR), Giza, Egypt

Abstract Cancer and antibacterial resistance threaten global health. Purine anti-cancer analogues are Nucleoside triphosphates and antimetabolites compete for DNA/RNA synthesis. new Pyrazolo[1,5-a]pyrimidine (5a-b) compounds were synthesized to test their antibacterial efficacy in vitro against microbial species, but give no activity Compared to 4 mg/mL Gentamycin (13mm and 11mm inhibition zones). In vitro antitumor activity of **5a-b** against A-549 lung carcinoma and HL-60 promyelocytic Leukemia showed significant CDK2 and CDK9 inhibition (14.40±0.69 and 16.27 ±0.71 µM, respectively). The SwissADME database assessed the molecule's pharmacokinetic, drug-like, and physicochemical properties. Drug-likeness is confirmed by all compounds following Veber rule in molecular properties. All compounds had 0.55 bioavailability radar scores. Except for. 5b have one Pain and 3 Brenk alerts. Unlike the 5a, Ninec has no Pain and two Brenk alerts. Thus, CDK2 and CDK9 inhibitors may treat proliferative disorders. these compounds inhibit CDK ENZYME, indicating good digestion. Our study found a powerful novel molecule that could improve anti-tumor treatments.

Keywords Pyrazolo[1,5-a]pyrimidine; Antimicrobial activity; Anticancer activity; CDK2; CDK9; A-549 and HL-60 cell line.

1. Introduction

An anticancer and antibacterial chemical may prevent bacterial infections during cancer treatment. Few studies have examined how these two approaches can fight infections and tumors. These therapies may weaken mucosal barriers, increasing bacterial infection risk [1]. In particular, Staphylococcus aureus affects cancer outcomes [2].

The pyrazolo[1,5-a]pyrimidine scaffold is needed for medicinal compound synthesis [3–4]. Pyrazo[1,5-a]pyrimidine-based purines fight cancer [5, 6, 7]. Pyrazo[1,5-a]pyrimidine derivatives inhibit CDK proteins, reducing tumor growth [8-9]. Dinaciclib, Roscovitine, and potential anticancer pyrazolo[3,4-d]pyrimidine leads are extensively researched in Figure 1. Type I CDK2 inhibitor dinaciclib inhibits CDK1, CDK5, and CDK9 at nanomolar levels. Dinaciclib beat flavopiridol and roscovitine in preclinical and clinical trials. Studies inhibit leukemia cell growth [10, 11]. Pharmacokinetics, safety, and efficacy were good [12, 13].

In this study, our objective was to synthesize a new series of pyrazolo[1,5-a]pyrimidines 5a-b, as purine analogues. These compounds have been previously investigated for their chemistry and anticancer properties. We aimed to

evaluate their antimicrobial activity against six microbial species and their anticancer activity against three human cancer cell lines. Moreover, the active compounds are subjected to molecular docking investigations inside the active site of CDK2 and CDK9, alongside an evaluation of the ADME features of the recently synthesized compounds.

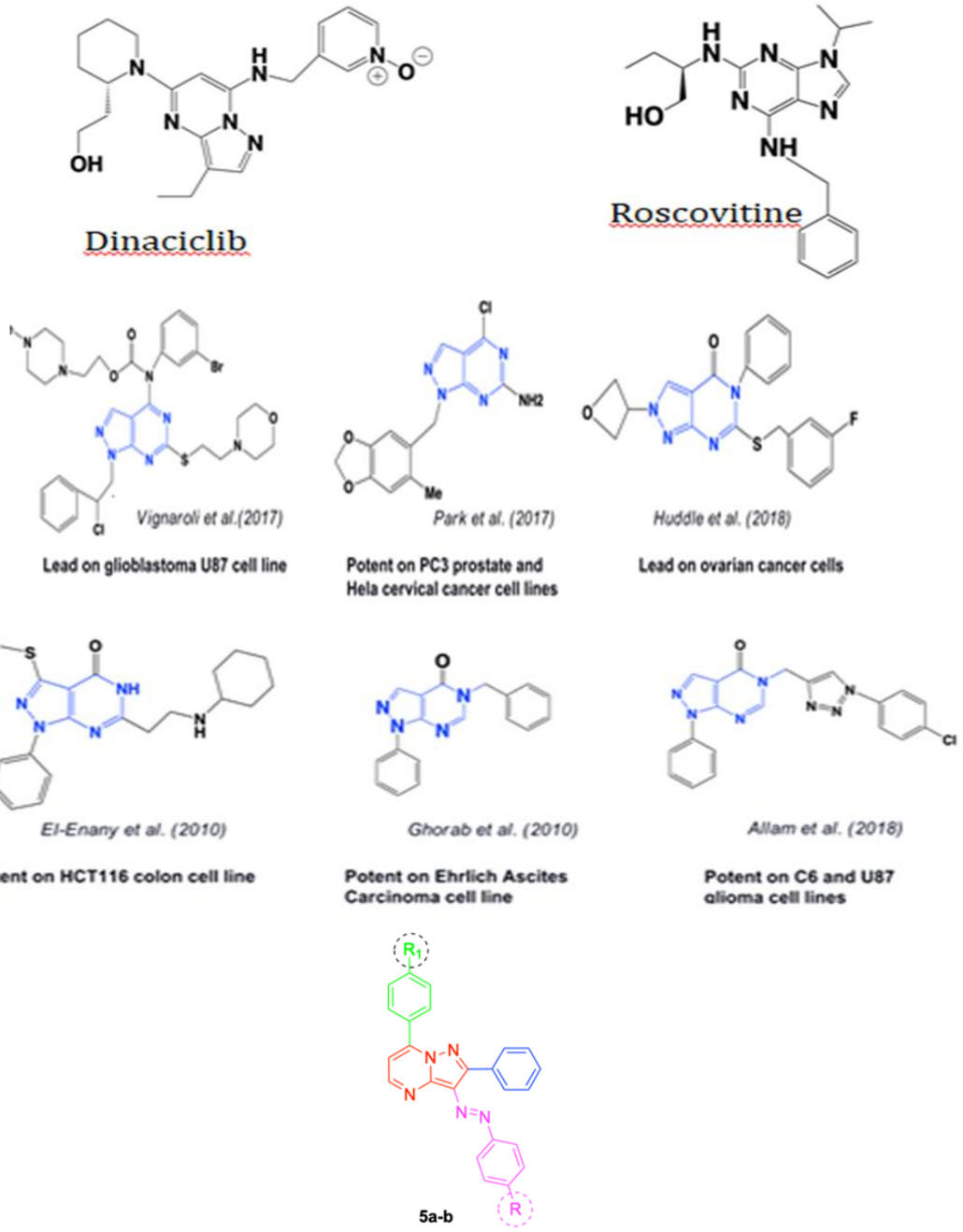

Figure: 1 Potential anticancer pyrazolo-pyrimidine leads and the new compound of Pyrazolo[1,5-a]pyrimidine

2. Results and Discussion

2.1. Molecular Properties

Physicochemical Properties

In-Silico SwissADME predictions for 5a-5b physiological and pharmacokinetic features: Small molecule therapeutic action relies on attaining the intended target at the right concentration, as described by ADME qualities. Lipinski's rule-of-five indicates tiny molecules may be drug-like. SwissADME quickly but accurately predicts a small molecule's physicochemical parameters (molecular weight, partition coefficient, solubility, topological surface area, etc.), pharmacokinetics, and druglikeness [14]. This method may anticipate lead compounds with drug-like qualities and change or improvise a molecule to have all the needed features. Thus, we predicted these properties of our newly developed molecules 5a-5b using SwissADME model.

Data obtained from this web tool suggested that all compounds obey Veber rule (Table 1) with zero violations indicative of their drug-likeliness. 5a and 5b compounds have 1 violation in Lipinski's rule of five.

Pharmacokinetic Properties

All compounds had clogP values between 4.00 and 6.50. Total polar atom surface area in a molecule is measured by Topological Polar Surface Area (TPSA). The acceptable TPSA range is typically 20-130 Å2. Note that all of our compounds were within this acceptable range. Solubility is low for all chemicals. None of the compounds crossed the blood-brain barrier. P-glycoprotein (P-gp) is an efflux transporter that actively removes xenobiotics from cells [15]. All compounds had P-gp non-substrate properties. All substances had 0.55 bioavailability. Chemicals absorb poorly in the gut. The 5b compounds have one Pain and three Brenk warnings, while the 5a compounds have one Pain and one Brenk alert.

Table 1: SwissADME prediction of physicochemical properties and bioavailability of compounds 5a-5b:

Molecule	5a	5b
Fraction Csp3	0	0
#Rotatable bonds	4	5
#H-bond acceptors	4	6
#H-bond donors	0	0
MR	127.19	128.31
TPSA	54.91	100.73
Consensus Log P	6.14	4.93
ESOL Class	Poorly soluble	Poorly soluble
GI absorption	Low	Low
BBB permeant	No	No
Pgp substrate	No	No
Lipinski #violations	1	1
Veber #violations	0	0
Bioavailability Score	0.55	0.55
PAINS #alerts	1	1
Brenk #alerts	1	3

SwissADME provides an intrinsic model known as BOILED-Egg for the purpose of predicting blood-brain barrier (BBB) permeability and passive gastrointestinal absorption (HIA). This approach is considered to be very effective, relying on two specific descriptors, notably WLOGP (representing lipophilicity) and TPSA (indicating apparent polarity). The presence of a white zone in the boiled egg is suggestive of a heightened likelihood of passive absorption via the gastrointestinal system, but the yellow region indicates a higher potential for reaching the brain. P-glycoprotein (P-gp) is an efflux pump involved in multidrug resistance, specifically responsible for the clearance of drugs. The BOILEDEgg plot utilizes a color-coded system to identify the P-glycoprotein (PGP) status of the drug candidate. Specifically, blue dots represent PGP+ drug candidates, while red dots represent PGP- drug candidates [16].

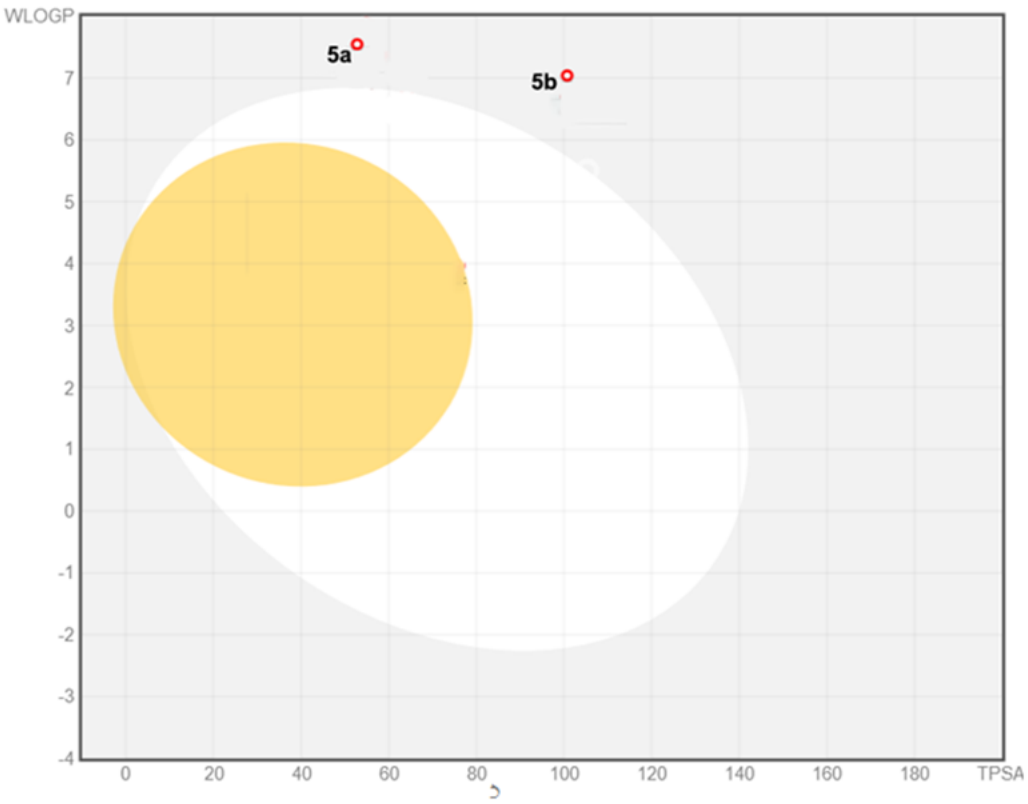

Figure 3: Spread of 5a-5b compounds on the BOILED-Egg plot

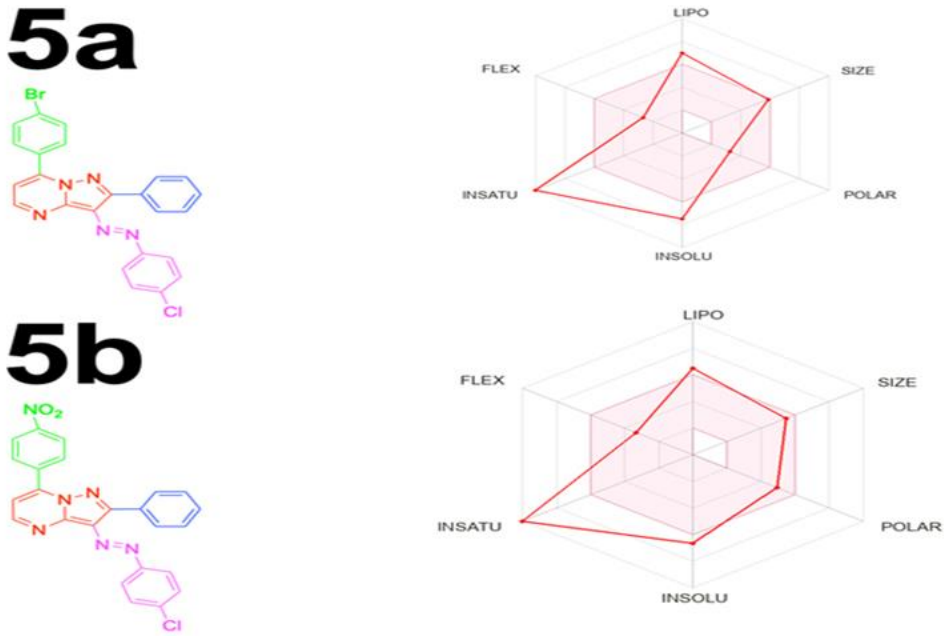

Figure 4: The bioavailability radar of derivative 5a and 5b

The spread of 5a-5b on BOILED-Egg is shown in Figure 3. It was observed that all compounds are non-BBB penetrant. the compounds were found outside the white region which indicates poor GI absorption. Among all compounds, all compounds were predicted to be not substrate for P-gp (PGP-) (red dot).

2.2. Analogue-based design through molecular docking studies

In light of the encouraging kinase inhibitory activity shown by the purine derivatives discussed in this work, a molecular docking analysis was conducted to investigate the binding interactions of the most potent derivatives 5a with the binding sites of the kinases under examination. The utilization of the molecular operating environment (MOE) 2019.02 facilitated the execution, examination, and depiction of the complete docking investigations. The 3-dimensional structural coordinates of CDK2 and CDK9 were obtained by downloading the data from the Protein Data Bank, specifically using the PDB IDs 3tnw and 3tn8, respectively. The chosen PDB IDs, namely 3tnw and 3tn8, exhibit high resolution values of 2 Å and 2.95 Å, respectively. Furthermore, it is worth noting that 3tnw and 3tn8 exhibit the presence of CDK2 and CDK9, which are bound to the powerful inhibitor CAN508. This characteristic renders them very suitable candidates for conducting docking experiments aimed at investigating their potential anticancer activity. The pose retrieval process for the co-crystallized ligands yielded distances of 0.265 and 0.4337 Å between the docked poses and the co-crystallized poses for CAN508. The provided diagram is seen in Figure 5.

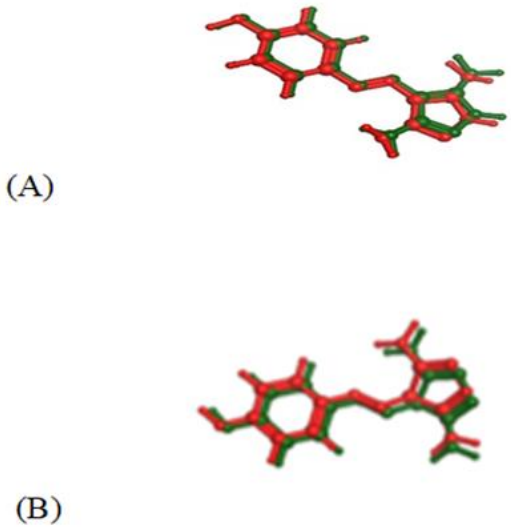

Figure 5: Superimposition of the co-crystallized (red) and the docking pose (green) of CAN508 in the CDK2 (A), CAN508 in the CDK9 (B)

In addition, the previous step produced an energy score (S) of -11.7195 for CAN508 in CDK2 and -10.045 for CAN508 in CDK9. These scores were negative. The docking scores that were retrieved from the co-crystallized ligands were used as a benchmark for comparing the values of compound 5a's docking score to those of other compounds.

2.3.1. Docking of compounds 5a into CDK2 active site

The examination of the interaction between CAN508 and the CDK2 active site through visual inspection indicated the establishment of two hydrogen bonds with the crucial residues Asp145 and Leu83. Furthermore, the observation of two pi-hydrogen bonds was made with Val18 and Leu134 (Figure 6).

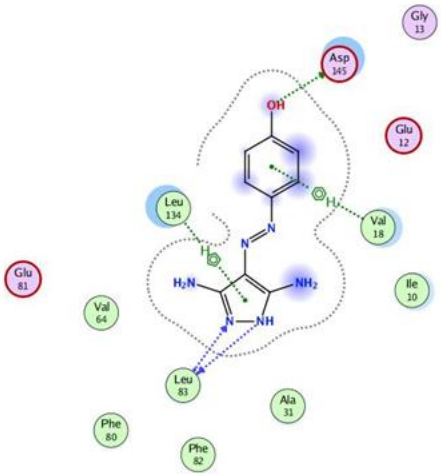

Figure 6: 2D diagram for the binding of CAN508 in the CDK2 active site (PDB: 3tnw)

Purine derivatives 5a fit well into the CDK2 active site with docking scores (-12.5367 kcal/mol) comparable to CAN508 (-11.7195). Compound 5a's binding patterns match CAN508's crystallographic binding mode in the CDK2-TK active site (PDB: 3tnw), Figure 7.

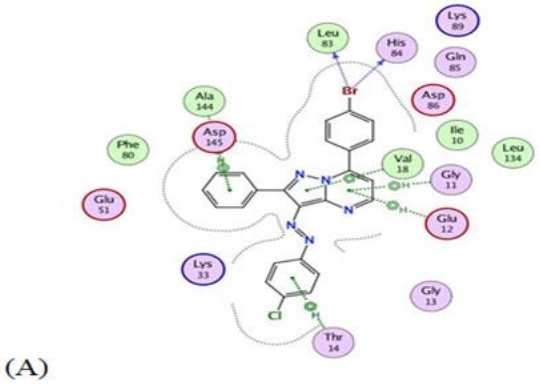

(A)

Figure 7: 2D diagram for the binding interactions of compound 5a (A) (PDB: 3tnw)

For instance, 5a compound forms 2 hydrogen bonds with Leu83 and His84 and 5 pi-hydrogen interactions with Ala144, Val18, Gly11, Glu12, and Thr14, indicating good CDK2 binding site fit. FIGURES 7 AND 8.

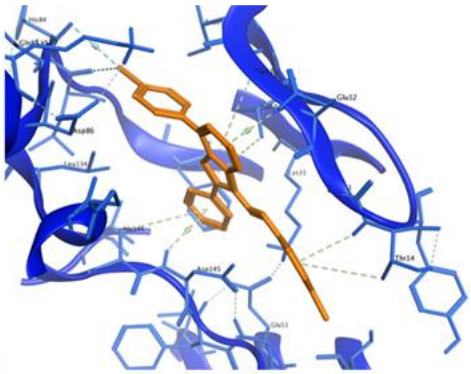

(A)

Figure 8: 3D diagram for the binding interactions of compound 5a (A) in the CDK2 active site (PDB: 3tnw)

2.3.2. Docking of compounds 5a into CDK9 active site

The good docking scores (-10.3325 kcal/mol) of compound 5a showed its efficient CDK9 inhibitory activity, comparable to CAN508 (-10.045). Figure 6 shows how CAN508 inhibits CDK9 by hydrogen bonding with Lys48 and pi-hydrogen interacting with Val33.

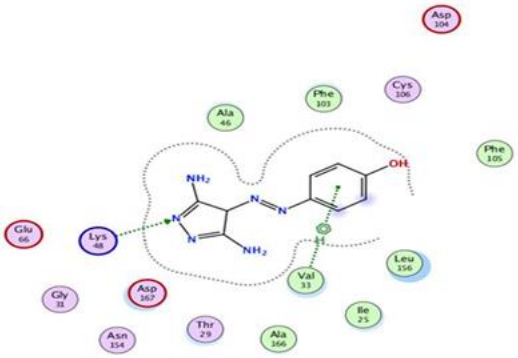

Figure 9: 2D diagram for the binding of CAN508 in the CDK9 active site (PDB: 3tn8)

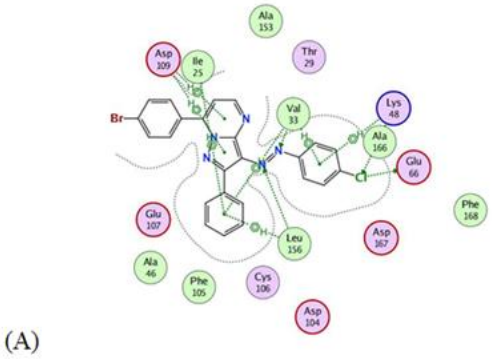

Figure 10: 2D diagram for the binding interactions of compound 5a (A) in the CDK9 active site (PDB: 3tn8)

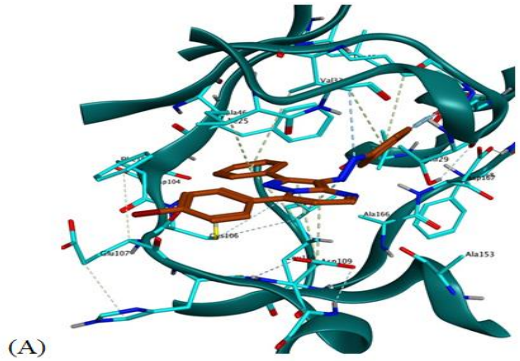

Figure 11: 3D diagram for the binding interactions of compound 5a (A) in the CDK9 active site (PDB: 3tn8)

Compound 5a docked into CDK9 active site and maintained multiple essential interactions (Figures 10 and 11).

In the CDK9 binding site, the 5a compound forms 4 hydrogen bonds with Lys48, Val33, and Glu66 residues and 7 pi-hydrogen interactions with Val33, Lys48, Leu156, Ile25, and Asp109, indicating good fit. Diagrams 10 and 11.

2.2. Chemistry

This research comprises the synthesis of novel pyrazolo[1,5-a]pyrimidine (5a-b) and compounds using the synthetic routes shown in Scheme 1. All of the target compounds' chemical structures were determined using proper elemental microanalyses as well as IR, Mass, and NMR spectrum data. In scheme 1, benzoylacetontrile was prepared and

converted to arylhyrazono-oxo-phenylpropane-nitriles which then treated with hydrazine hydrate in ethanol to afford 5-amino-4-arylzo-3-phenylpyrazoles 1a, b [17], subsequently they reacted with different Enaminones 2a-f which were prepared by the reaction of acetophenones with N,N-dimethylformamide dimethylacetal [18] to yield tilted compounds 3a-b, afterwards they were cyclized under the influence of nucleophilic attack resulting in unstable compounds 4a-b that dehydrated rapidly to yield 5a-b. The 1HNMR data of compounds 5a-b revealed no presence of distinct peak of methyl proton.

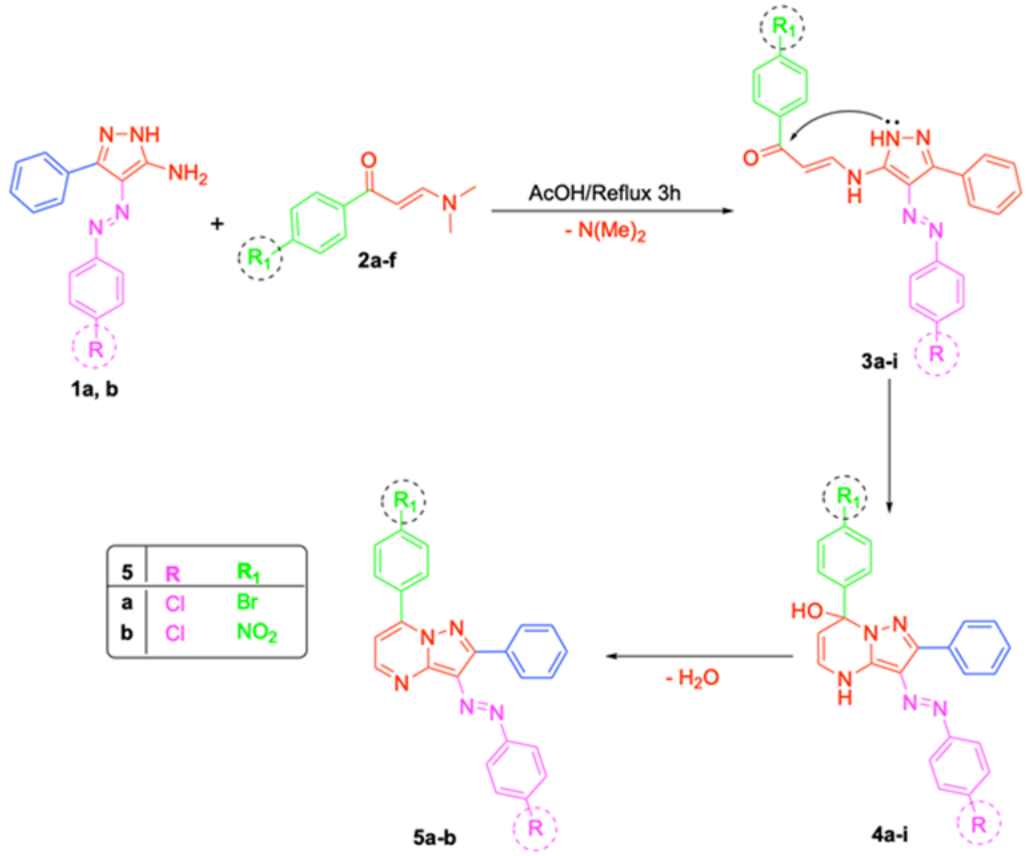

Scheme 1**: Synthesis of pyrazolo[1,5-a]pyrimidine derivatives **5a-b

2.3. Biological activity

2.3.1. In vitro Antimicrobial Evaluation

The synthesized compounds displayed significant antimicrobial potential on selected pathogenic bacteria whereas show resistance against tested fungi as shown in table 2.

Table 2: Antimicrobial activity by well diffusion method for different extracted compounds against pathogenic microbes.

Item		5a	5b	Gentamicin	Ketoconazole
Staphylococcus aureus	ATCC 25923	NA	NA	24	
Bacillus subtilis	RCMB 015 (1) NRRL B-543	NA	NA	26	
Escherichia coli ATCC 25922		NA	NA	30	
Proteus vulgaris	RCMB 004 (1) ATCC 13315	NA	NA	25	
Aspergillus fumigatus	(RCMB 002008)	NA	NA		17
Candida albicans	RCMB 005003 (1) ATCC 10231	NA	NA		20

It was observed from results that:
The compounds (5a-5b) not showed any antimicrobial activity (no p-value) on selected pathogenic bacteria gram positive and negative and not recorded antimicrobial activity against tested fungi Aspergillus fumigatus and Candida albicans.

2.3.2. In vitro Cytotoxic Activity Evaluation

The management of a human breast cancer cell line the MCF-7 and A-549 cell lines are commonly used in academic research. Lung carcinoma and HL-60 promyelocytic Leukemia exhibited notable anti-tumor efficacy when exposed to varying concentrations of synthesized compounds, resulting in the suppression of growth at distinct IC50 values in comparison to the reference drug Cisplatin (Table 1). Based on the IC50 values obtained for compounds 5a and 5b, it can be inferred that the inclusion of a pyrazol ring, as well as the presence of Pyrazolo[1,5-a]pyrimidine, resulted in the highest level of activity. Specifically, compound 5a exhibited an IC50 value of 14.40 ±0.69 µM against Lung carcinoma cells, which is comparable to the activity of Cisplatin (IC50 = 7.48 ±0.56 µM). Additionally, compound 5a demonstrated an IC50 value of 7.19 ±0.34 µM against promyelocytic Leukemia, which is similar to the activity of Cisplatin (IC50 = 16.75 ±0.91 µM). Upon analyzing the substitutions at positions 1 and 5 of the pyrazolo[1,5-a]pyrimidine moiety, it was observed that the pyrimidine derivative 5a, which contained bromobenzene at position 2 of the pyrazolo[1,5-a]pyrimidine, exhibited IC50 values of 14.40 ±0.69 and 16.75 ± 0.91 µM, respectively (as shown in Table 1).

Item	Lung carcinoma	Breast carcinoma	promyelocytic Leukemia
5a	**14.40 ±0.69**	30.77 ±0.81	16.27 ±0.71
5b	**72.05 ± 5.13**	109.21± 6.27	107.40 ± 6.89
Cisplatin	**7.48** ± **0.56**	5.67 ± 0.45	16.75 ± 0.91

3. Conclusion

A novel series of Pyrazolo[1,5-a]pyrimidine derivatives (5a-b) was synthesized employing 5-amino-4-arylzo-3-phenylpyrazoles (1a,b) as initial substrates. Subsequently, docking studies were conducted to forecast their potential as anti-cancer agents. Subsequently, the recently synthesized compounds underwent in vitro testing to evaluate their antimicrobial and anticancer properties. A total of six microbial species were subjected to experimentation in order to evaluate their antimicrobial properties against specific target compounds. The anticancer efficacy of the compound was also evaluated on A-549 lung carcinoma, HL-60 promyelocytic leukemia, and MCF-7 cell lines. The study suggests that the incorporation of bromobenzene at position 2 of Pyrazolo[1,5-a]pyrimidine derivatives leads to enhanced anticancer properties. The derivatives of Pyrazolo[1,5-a]pyrimidine 5a-b exhibited a lack of antibacterial activity when compared to the reference drugs. The compound pyrazolo[1,5-a]pyrimidine 5a exhibited the most pronounced cytotoxic effects on A-549 lung carcinoma and HL-60 promyelocytic leukemia cell lines. According to the findings of this study, it is suggested that Pyrazolo[1,5-a]pyrimidine-based compounds possess the potential to produce antimicrobial and anticancer derivatives of enhanced potency, subject to additional investigation.

4. Experimental

4.1. Molecular properties prediction

In-Silico SwissADME predictions
SwissADME is an online utility that is widely recognized for its reliability and availability for free [19]

4.2. Molecular docking studies

All the minimizations were performed with MOE until a RMSD gradient of 0.05 kcal mol-1 Å-1 with MMFF94X forcefield and the partial charges were automatically calculated.

4.3. Chemistry

4.3.1. General

Melting points (°C, uncorrected) were determined using a Stuart melting point apparatus. The IR spectra (KBr) were recorded on a SHIMADZU FT/IR spectrometer. The NMR spectra recorded by BRUKER 400 MHz NMR spectrometers. Chemical shifts were reported in parts per million (δ), and coupling constants (J) expressed in Hertz. TMS was used as an internal standard and chemical shifts were measured in d ppm. 1H and 13C spectra were run at 400 and 100 MHz, respectively. were prepared according to the reported method. 3-phenyl-4-(4-tolyldiazenyl)-1H-pyrazol-5-amine (1a) and 4-((4-chlorophenyl)diazenyl)-3-phenyl-1H-pyrazol-5-amine (1b) [1], 3-(dimethylamino)-1-arylprop-2-en-1-ones 2a-f [2], 3-oxo-3-phenylpropanenitrile [20], 3-oxo-3-phenylpropanenitrile [21] and 3-phenyl-1H-pyrazol-5-amine [22] were prepared according to the reported methods.

4.3.2. General procedure for the synthesis of pyrazolo[1,5-a]pyrimidines 5a-b

A mixture of 3-phenyl-4-(aryldiazenyl)-1H-pyrazol-5-amine 1a, b (1 mmol) and the appropriate 3-(dimethylamino)-1-arylprop-2-en-1-ones 2a-f (1 mmol) in glacial acetic acid (15 mL) was heated under reflux for 3 h. The formed precipitate was filtered, washed with ethanol, and recrystallized from EtOH/DMF to furnish the corresponding pyrazolo[1,5-a]pyrimidines 5a-b, respectively.

4.3.2.1.7-(4-Bromophenyl)-3-((4-chlorophenyl)diazenyl)-2-phenylpyrazolo[1,5-a]pyrimidine (5a)

Orange powder, 70% yield; mp 181-183oC; IR (KBr) νmax/cm-1 1705, 1589 (C=C), 1539, 1485 (C=N). 1H NMR (DMSO-d6) δ 7.51-7.59 (m, 4H, ArH), 7.60 – 7.67 (m, 2H, ArH), 7.78 – 7.85 (m, 2H, ArH), 7.89 (d, J = 8.5 Hz, 2H, ArH), 8.15-8.18 (m, 4H, ArH), 8.92 (d, J = 4.5 Hz, 1H, ArH). 13C NMR (DMSO-d6) δ 111.49, 123.79 (2C), 125.20, 125.65, 129.07 (2C), 129.50, 129.91 (2C), 129.94 (2C), 130.12, 131.96, 132.14 (2C), 132.44 (2C), 134.77, 140.02, 145.57, 152.71, 154.14, 154.48. MS m/z (%) 490.55 (M++2, 45.69), 489.48 (M++2, 14.90), 488.83 (M+, 47.52), 368.21 (100). Anal. Calcd. For: C24H15BrClN5 (488.77): C, 58.98; H, 3.09; N, 14.33; found: C, 59.12; H, 3.23; N, 14.50

4.3.2.2.3-((4-Chlorophenyl)diazenyl)-7-(4-nitrophenyl)-2-phenylpyrazolo[1,5-a]pyrimidine (5b)

Red powder, 85% yield; mp 230-232oC; IR (KBr) νmax/cm-1 1720, 1589 (C=C), 1520 (C=N). 1H NMR (DMSO-d6) δ 7.48 – 7.67 (m, 6H), 7.78 – 7.86 (m, 2H), 8.12 – 8.19 (m, 2H), 8.42 – 8.52 (m, 4H), 8.96 (d, J = 4.4 Hz, 1H). 13C NMR (DMSO-d6) δ 112.21, 123.82 (2C), 124.02 (2C), 125.30, 129.07 (2C), 129.91 (2C), 129.95 (2C), 130.16, 131.84, 131.97 (2C), 134.88, 136.39, 139.90, 144.48, 149.26, 152.66, 154.15, 154.54. MS m/z (%) 455.65 (M+ +1, 11.82), 454.00 (M+, 30.65), 239.30 (100). Anal. Calcd. For: C24H15ClN6O2 (454.87): C, 63.37; H, 3.32; N, 18.48; found: C, 63.45; H, 3.51; N, 18.63.

4.4. Biological Activity

4.4.1. Materials and methods

4.4.1.1. Antimicrobial activity

Antimicrobial potential of tested compounds was determined by using Agar well-diffusion method. [23].

4.4.1.2. In Vitro Cytotoxicity Screening

4.4.1.2.1. Chemicals

Dimethyl sulfoxide (DMSO), Fetal Bovine serum, MTT and trypan blue dye were purchased from Sigma (St. Louis, Mo., USA). RPMI-1640, HEPES buffer solution, L-glutamine, gentamycin and 0.25% Trypsin-EDTA were purchased from Lonza (Belgium).

4.3.1.2.2. Cell Culture

Mammalian cell lines: MCF-7 cells (human breast cancer cell line), A-549 cells (human lung carcinoma cell line) and HL-60 cells (human promyelocytic Leukemia cell line) were obtained from the American Type Culture Collection (ATCC, Rockville, MD).

Cell line Propagation

The cells were grown on RPMI-1640 medium supplemented with 10% inactivated fetal calf serum and 50µg/ml gentamycin. The cells were maintained at 37ºC in a humidified atmosphere with 5% CO2 and were subcultured two to three times a week.

4.3.1.2.3. *In vitro* cytotoxic assay

Anti-cancer activities were done using MTT colorimetric assay. Cell viability was assessed after 48 h and the viability was calculated relative to control [24].

References

[1]. Rolston KVI. Infections in Cancer Patients with Solid Tumors: A Review. Infectious Diseases and Therapy [Internet] 2017 3;6:69–83. doi: http://dx.doi.org/10.1007/s40121-017-0146-1doi: 10.1007/s40121-017-0146-1

[2]. Greco C, Catania R, Balacco DL, Taresco V, Musumeci F, Alexander C, et al. Synthesis and Antibacterial Evaluation of New Pyrazolo[3,4-d]pyrimidines Kinase Inhibitors. Molecules [Internet] 2020 16;25:5354. doi: http://dx.doi.org/10.3390/molecules25225354doi: 10.3390/molecules25225354

[3]. Abdelhamid AO, Gomha SM, El-Enany WAMA. Efficient Synthesis and Antimicrobial Evaluation of New Azolopyrimidines-Bearing Pyrazole Moiety. Journal of Heterocyclic Chemistry [Internet] 2019 29;56:2487–93. doi: http://dx.doi.org/10.1002/jhet.3638doi: 10.1002/jhet.3638

[4]. Abbas IM, Abdallah MA, Gomha SM, Kazem MSH. Synthesis and Antimicrobial Activity of Novel Azolopyrimidines and Pyrido-Triazolo-Pyrimidinones Incorporating Pyrazole Moiety. Journal of Heterocyclic Chemistry [Internet] 2017 13;54:3447–57. doi: http://dx.doi.org/10.1002/jhet.2968doi: 10.1002/jhet.2968

[5]. Gomha S, Farghaly T, Mabkhot Y, Zayed M, Mohamed A. Microwave-Assisted Synthesis of some Novel Azoles and Azolopyrimidines as Antimicrobial Agents. Molecules [Internet] 2017 23;22:346. doi: http://dx.doi.org/10.3390/molecules22030346doi: 10.3390/molecules22030346

[6]. Cherukupalli S, Karpoormath R, Chandrasekaran B, Hampannavar GirishA, Thapliyal N, Palakollu VN. An insight on synthetic and medicinal aspects of pyrazolo[1,5-a]pyrimidine scaffold. European Journal of Medicinal Chemistry [Internet] 2017;126:298–352. doi: http://dx.doi.org/10.1016/j.ejmech.2016.11.019doi: 10.1016/j.ejmech.2016.11.019

[7]. Ismail NSM, Ali GME, Ibrahim DA, Elmetwali AM. Medicinal attributes of pyrazolo[1,5-a]pyrimidine based scaffold derivatives targeting kinases as anticancer agents. Future Journal of Pharmaceutical Sciences [Internet] 2016;2:60–70. doi: http://dx.doi.org/10.1016/j.fjps.2016.08.004doi: 10.1016/j.fjps.2016.08.004

[8]. Li Y, Gao W, Li F, Wang J, Zhang J, Yang Y, et al. An in silico exploration of the interaction mechanism of pyrazolo[1,5-a]pyrimidine type CDK2 inhibitors. Molecular BioSystems [Internet] 2013;9:2266. doi: http://dx.doi.org/10.1039/c3mb70186gdoi: 10.1039/c3mb70186g

[9]. Williamson DS, Parratt MJ, Bower JF, Moore JD, Richardson CM, Dokurno P, et al. Structure-guided design of pyrazolo[1,5-a]pyrimidines as inhibitors of human cyclin-dependent kinase 2. Bioorganic & Medicinal Chemistry Letters [Internet] 2005;15:863–7. doi: http://dx.doi.org/10.1016/j.bmcl.2004.12.073doi: 10.1016/j.bmcl.2004.12.073

[10]. Heathcote DA, Patel H, Kroll SHB, Hazel P, Periyasamy M, Alikian M, et al. A Novel Pyrazolo[1,5-a]pyrimidine Is a Potent Inhibitor of Cyclin-Dependent Protein Kinases 1, 2, and 9, Which Demonstrates Antitumor Effects in Human Tumor Xenografts Following Oral Administration. Journal of Medicinal Chemistry [Internet] 2010 16;53:8508–22. doi: http://dx.doi.org/10.1021/jm100732tdoi: 10.1021/jm100732t

[11]. Kamal A, Tamboli JR, Nayak VL, Adil SF, Vishnuvardhan MVPS, Ramakrishna S. Synthesis of pyrazolo[1,5-a]pyrimidine linked aminobenzothiazole conjugates as potential anticancer agents. Bioorganic

& Medicinal Chemistry Letters [Internet] 2013;23:3208–15. doi: http://dx.doi.org/10.1016/j.bmcl.2013.03.129doi: 10.1016/j.bmcl.2013.03.129

[12]. Park SJ, Kim E, Yoo M, Lee J-Y, Park CH, Hwang JY, et al. Synthesis and biological evaluation of N9-cis-cyclobutylpurine derivatives for use as cyclin-dependent kinase (CDK) inhibitors. Bioorganic & Medicinal Chemistry Letters [Internet] 2017;27:4399–404. doi: http://dx.doi.org/10.1016/j.bmcl.2017.08.018doi: 10.1016/j.bmcl.2017.08.018

[13]. Zhao H, Li S, Wang G, Zhao W, Zhang D, Wang F, et al. Study of the mechanism by which dinaciclib induces apoptosis and cell cycle arrest of lymphoma Raji cells through a CDK1-involved pathway. Cancer Medicine [Internet] 2019 17;8:4348–58. doi: http://dx.doi.org/10.1002/cam4.2324doi: 10.1002/cam4.2324

[14]. Roskoski R. Cyclin-dependent protein serine/threonine kinase inhibitors as anticancer drugs. Pharmacological Research [Internet] 2019;139:471–88. doi: http://dx.doi.org/10.1016/j.phrs.2018.11.035doi: 10.1016/j.phrs.2018.11.035

[15]. Parry D, Guzi T, Shanahan F, Davis N, Prabhavalkar D, Wiswell D, et al. Dinaciclib (SCH 727965), a Novel and Potent Cyclin-Dependent Kinase Inhibitor. Molecular Cancer Therapeutics [Internet] 2010 1;9:2344–53. doi: http://dx.doi.org/10.1158/1535-7163.mct-10-0324doi: 10.1158/1535-7163.mct-10-0324

[16]. Saqub H, Proetsch-Gugerbauer H, Bezrookove V, Nosrati M, Vaquero EM, de Semir D, et al. Dinaciclib, a cyclin-dependent kinase inhibitor, suppresses cholangiocarcinoma growth by targeting CDK2/5/9. Scientific Reports [Internet] 2020 28;10. doi: http://dx.doi.org/10.1038/s41598-020-75578-5doi: 10.1038/s41598-020-75578-5

[17]. Shawali AS, Abdelkader MH, Eltalbawy FMA. Synthesis and tautomeric structure of novel 3,7-bis(arylazo)-2,6-diphenyl-1H-imidazo-[1,2-b]pyrazoles in ground and excited states. Tetrahedron [Internet] 2002;58:2875–80. doi: http://dx.doi.org/10.1016/s0040-4020(02)00157-6doi: 10.1016/s0040-4020(02)00157-6

[18]. Lin Y-I, Lang SA. New synthesis of isoxazoles and isothiazoles. A convenient synthesis of thioenaminones from enaminones. The Journal of Organic Chemistry [Internet] 1980;45:4857–60. doi: http://dx.doi.org/10.1021/jo01312a011doi: 10.1021/jo01312a011

[19]. Daina A, Zoete V. A BOILED-Egg To Predict Gastrointestinal Absorption and Brain Penetration of Small Molecules. ChemMedChem [Internet] 2016 24;11:1117–21. doi: http://dx.doi.org/10.1002/cmdc.201600182doi: 10.1002/cmdc.201600182

[20]. Petek N, Štefane B, Novinec M, Svete J. Synthesis and biological evaluation of 7-(aminoalkyl)pyrazolo[1,5-a]pyrimidine derivatives as cathepsin K inhibitors. Bioorganic Chemistry [Internet] 2019;84:226–38. doi: http://dx.doi.org/10.1016/j.bioorg.2018.11.029doi: 10.1016/j.bioorg.2018.11.029

[21]. Ji Y, Trenkle WC, Vowles JV. A High-Yielding Preparation of β-Ketonitriles. Organic Letters [Internet] 2006 23;8:1161–3. doi: http://dx.doi.org/10.1021/ol053164zdoi: 10.1021/ol053164z

[22]. Saczewski J, Paluchowska A, Klenc J, Raux E, Barnes S, Sullivan S, et al. Synthesis of 4-substituted 2-(4-methylpiperazino)pyrimidines and quinazoline analogs as serotonin 5-HT2A receptor ligands. Journal of Heterocyclic Chemistry [Internet] 2009;46:1259–65. doi: http://dx.doi.org/10.1002/jhet.236doi: 10.1002/jhet.236

[23]. Andrews JM. Determination of minimum inhibitory concentrations. Journal of Antimicrobial Chemotherapy [Internet] 2001 1;48:5–16. doi: http://dx.doi.org/10.1093/jac/48.suppl_1.5doi: 10.1093/jac/48.suppl_1.5

[24]. Mosmann T. Rapid colorimetric assay for cellular growth and survival: Application to proliferation and cytotoxicity assays. Journal of Immunological Methods [Internet] 1983;65:55–63. doi: http://dx.doi.org/10.1016/0022-1759(83)90303-4doi: 10.1016/0022-1759(83)90303-4